

A model for free-radical reactions

Udo Höweler und Martin Klessinger

Organisch-Chemisches Institut der Universität, D-4400 Münster, Federal Republic of Germany

Using an EHT type Hamiltonian the Heitler-London-VB treatment of the three-centre three-electron problem is simplified such that the interesting features of the potential hypersurfaces of arbitrary three-centre three-electron systems can be obtained simply from the knowledge of atomic orbital energies and overlap integrals. The method is applied to the hypersurfaces of the H_3 system and extensions of the discussion of general radical reactions are indicated.

Key words: Potential energy hypersurfaces of H_3 —three-centre three-electron problem—unpolar radical reactions

1. Introduction

In a detailed comparison between the results of ab-initio and semiempirical model calculations for the H_3 system we deduced the requirements for a simple but reliable quantum chemical method to investigate radical reactions [1]. Based on the Heitler-London VB approach originally applied to the three-centre three-electron (3C3E) problem [2] by Bonačić-Koutecký et al. [3] we now present such a model which fulfills these requirements by taking into account overlap and electron correlation and which therefore should be particularly suited to describe unpolar radical reactions. From this model explicit expressions may be obtained which reproduce correctly the essential features of the potential energy hypersurfaces of a 3C3E model for arbitrary radical systems.

2. Results and discussion

In order to simplify the VB treatment of Ref. [3] we use an EHT type Hamiltonian

$$\mathcal{H}^{EH} = \sum_i h_{\text{eff}}(i). \quad (1)$$

From the Matrix representation $\langle \Phi_I | \mathcal{H}^{\text{EH}} | \Phi_J \rangle$ of this Hamiltonian in the basis of the two covalent structures

$$\Phi_1 = (|1\bar{2}3\rangle - |\bar{1}23\rangle) / \sqrt{2} \quad (2)$$

and

$$\Phi_2 = (2|\bar{1}23\rangle - |\bar{1}\bar{2}3\rangle - |12\bar{3}\rangle) / \sqrt{6} \quad (3)$$

and from the Wolfsberg-Helmholtz expression [4]

$$h_{\mu\nu} = \frac{1}{2}K(h_{\mu\mu} + h_{\nu\nu})S_{\mu\nu} \quad (4)$$

for the two-centre integrals $h_{\mu\nu} = \langle \mu | h_{\text{eff}} | \nu \rangle$ we obtain the secular equation

$$\begin{vmatrix} A + m_{23}S_{23}^2 - \frac{1}{2}(m_{12}S_{12}^2 + m_{13}S_{13}^2) - E(1 - \mathcal{S} + \sigma_1) & \frac{\sqrt{3}}{2}(m_{12}S_{12}^2 - m_{13}S_{13}^2) - E\sigma_2 \\ \frac{\sqrt{3}}{2}(m_{12}S_{12}^2 - m_{13}S_{13}^2) - E\sigma_2 & A - m_{23}S_{23}^2 + \frac{1}{2}(m_{12}S_{12}^2 + m_{13}S_{13}^2) - E(1 - \mathcal{S} - \sigma_1) \end{vmatrix} = 0 \quad (5)$$

where

$$A = h_{11} + h_{22} + h_{33} - h_{12}S_{13}S_{23} - h_{13}h_{12}S_{23} - h_{23}S_{12}S_{13} \quad (6)$$

$$m_{\mu\nu} = K(h_{\mu\mu} + h_{\nu\nu}) + h_{\kappa\kappa} \quad (7)$$

and

$$\mathcal{S} = S_{12}S_{13}S_{23}$$

$$\sigma_1 = \frac{1}{2}(2S_{23}^2 - S_{12}^2 - S_{13}^2) \quad (8)$$

$$\sigma_2 = S_{12}^2 - S_{13}^2.$$

Neglecting \mathcal{S} , σ_1 and σ_2 [1, 3] the roots of the secular equation may be written as

$$\begin{aligned} E_{I,II} &= A \pm \frac{|m_{12}|}{\sqrt{6}} \left\{ \left(S_{12}^2 - \frac{m_{23}}{m_{12}} S_{23}^2 \right)^2 + \left(S_{12}^2 - \frac{m_{13}}{m_{13}} S_{13}^2 \right)^2 \right. \\ &\quad \left. + \left(\frac{m_{23}}{m_{12}} S_{23}^2 - \frac{m_{23}}{m_{12}} S_{13}^2 \right)^2 \right\}^{1/2} \\ &= A \pm \varepsilon. \end{aligned} \quad (9)$$

The term ε which in contrast to Ref. [3] contains no two-electron terms, modulates the term A which makes the energy of both the lowest two doublet states increase with increasing overlap, i.e. with decreasing internuclear distances. This is to say, that maxima of the ground state energy $E_I = A + \varepsilon$ and minima of the excited state energy $E_{II} = A - \varepsilon$ occur at geometries where ε has its minima.

These geometries are obtained by setting $\partial\varepsilon/(\partial S_{\mu\nu}^2) = 0$ which yields

$$S_{12}^2 = \frac{1}{2} \left(\frac{m_{13}}{m_{12}} S_{13}^2 + \frac{m_{23}}{m_{12}} S_{23}^2 \right) \quad (10)$$

$$S_{13}^2 = \frac{1}{2} \left(\frac{m_{12}}{m_{13}} S_{12}^2 + \frac{m_{23}}{m_{23}} S_{23}^2 \right) \quad (11)$$

$$S_{23}^2 = \frac{1}{2} \left(\frac{m_{12}}{m_{23}} S_{12}^2 + \frac{m_{13}}{m_{23}} S_{13}^2 \right) \quad (12)$$

which all correspond to minima of ε since $\partial^2 \varepsilon / (\partial S_{\mu\nu}^2)^2 \geq 0$. Inserting Eq. (12) into Eq. (9) yields

$$\langle \Phi_1 | \mathcal{H}^{\text{EH}} | \Phi_1 \rangle = \langle \Phi_2 | \mathcal{H}^{\text{EH}} | \Phi_2 \rangle = A. \quad (13)$$

The structures Φ_1 and Φ_2 are degenerate and the splitting of the lowest two doublet states is entirely determined by the off-diagonal element

$$\langle \Phi_1 | \mathcal{H}^{\text{EH}} | \Phi_2 \rangle = \frac{\sqrt{3}}{2} (m_{12} S_{12}^2 - m_{13} S_{13}^2). \quad (14)$$

Thus the ground state is the more stabilized the larger the difference $m_{12} S_{12}^2 - m_{13} S_{13}^2$, i.e. the larger $m_{12} S_{12}^2$. Similar results may be obtained by inserting Eq. (10) or Eq. (11) into Eq. (9), but from these three sets of equations only two are linearly independent.

These simple formulae may be tested by comparison with ab-initio VB-CI calculations for the H_3 system. The potential energy hypersurfaces of the ground and the first excited state as calculated using an independently scaled and floated minimal basis set (STO-4G [15]) with the geometrical parameters ξ and η defined in Fig. 1 and R_{12} kept constant at 2.0 a.u. are shown in Fig. 2a and b, whereas in Fig. 2c the curves *a* and *b* are given which are determined by

$$S_{12}^2 = \frac{1}{2} (S_{13}^2 + S_{23}^2) \quad (15)$$

$$S_{23}^2 = \frac{1}{2} (S_{12}^2 + S_{13}^2). \quad (16)$$

and which divide up the coordinate space into the regions *A*, *B* and *C*.

Eq. (15) and Eq. (16) are obtained from Eq. (10) and Eq. (12) by setting $m_{12} = m_{13} = m_{23}$ corresponding to the fact that for homonuclear 3C3E systems like H_3 all one-centre energies $h_{\mu\mu}$ are identical.

It is evident that in Fig. 2c the curve *b* given by Eq. (16) describes surprisingly well the top of the potential ridge of the ground state hypersurface in Fig. 2a

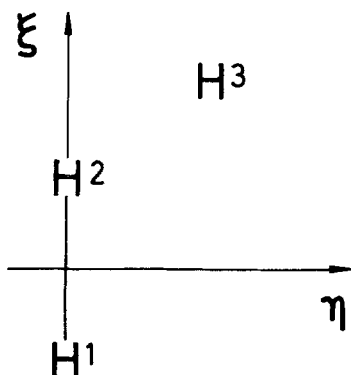


Fig. 1. Coordinate space for the H_3 system

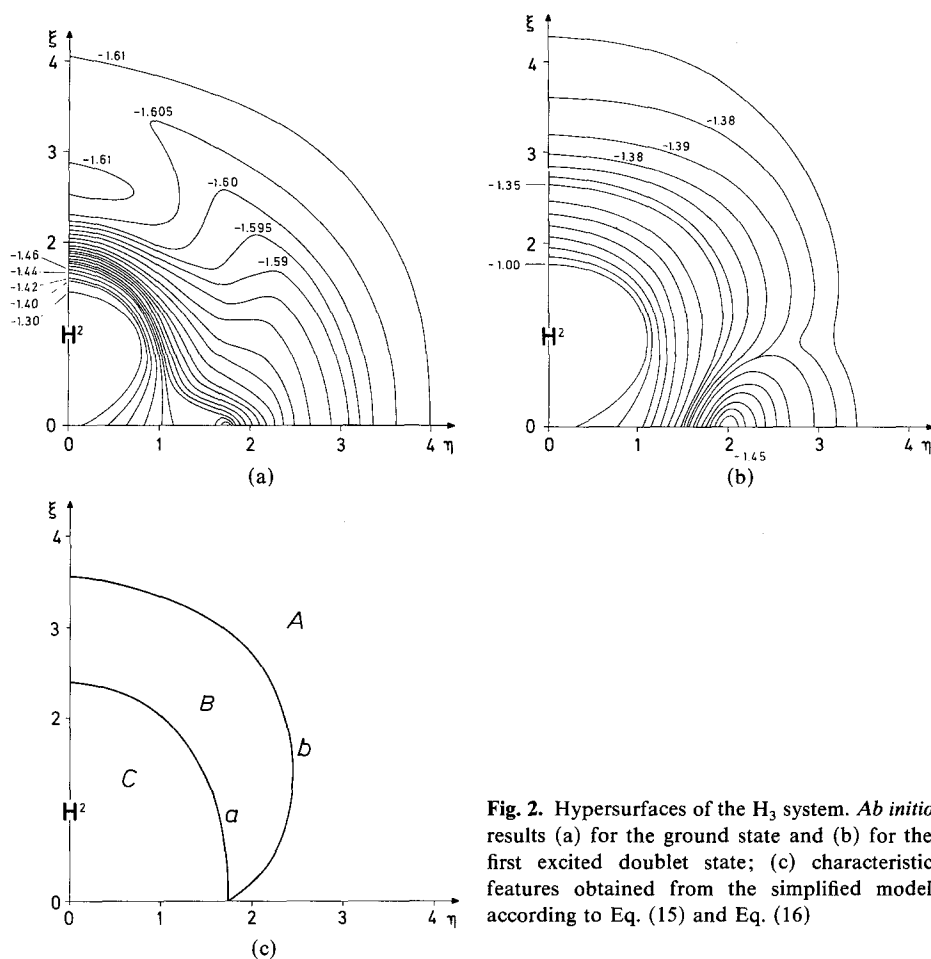


Fig. 2. Hypersurfaces of the H_3 system. *Ab initio* results (a) for the ground state and (b) for the first excited doublet state; (c) characteristic features obtained from the simplified model according to Eq. (15) and Eq. (16)

and the corresponding well of the excited state hypersurface in Fig. 2b, which extend from the upper left hand corner ($\xi = 3.5$, $\eta = 0$ a.u.) to the middle of the lower edge ($\xi = 0$, $\eta = 1.73$ a.u.). The fact that according to Eq. (14) ε decreases along this line is in good agreement with the increasing height of the ridge in Fig. 2a. The shallow well which leads on the ground state surface Fig. 2a from $\xi = 2.7$, $\eta = 0$ a.u. to $\xi = 0$, $\eta = 1.4$ a.u. lies in Fig. 2c between the curves a and b given by Eq. (15) and Eq. (16) and crosses these curves near the η -axis. Thus the main features of the hypersurfaces in Fig. 2a and Fig. 2b are correctly reproduced by the model and its simple form lends itself particularly well for a clear physical interpretation of the process of radical reactions.

Thus, according to Eq. (13) the structures Φ_1 and Φ_2 are degenerate along the curve b in Fig. 2c. In region A the ground state wave function is dominated by Φ_2 which describes the triplet coupling of the electron spins at centres 2 and 3, while in regions B and C Φ_1 dominates which describes their singlet coupling. Therefore curve b marks those geometries at which the characteristics of the

ground and excited state are exchanged and the new bond is formed. The corresponding barrier occurs due to the electron recoupling and its height is determined by the amount of mixing between the two structures.

The curve *a* in Fig. 2c is easily understood if instead of Φ_1 and Φ_2 the two structures

$$\Phi'_1 = (|1\bar{2}3\rangle - |\bar{1}23\rangle)/\sqrt{2} \quad (17)$$

and

$$\Phi'_2 = (2|12\bar{3}\rangle - |\bar{1}23\rangle - |1\bar{2}3\rangle)/\sqrt{6} \quad (18)$$

are used, which are connected to Φ_1 and Φ_2 by a unitary transformation. The ground state wave function is dominated in regions *A* and *B* by Φ'_1 , which describes the singlet coupling of the electron spins at the initially bounded centres 1 and 2, and in region *C* by Φ'_2 , which describes their antibonding triplet coupling. Therefore curve *a*, along which these two structures are degenerate, marks those geometries at which the switchover from the bonding to the antibonding electron coupling occurs and the initial bond is broken. During addition reactions the curve *b* in Fig. 2c has to be crossed in order to form the new bond, but for non-perpendicular attacks the curve *a* is never touched, so that the initial bond is not affected; during the perpendicular attack on the other hand both curves have to be crossed simultaneously. Thus the transition state geometries may be described as follows: The initial bond remains essentially unperturbed in the linear attack while it will be stretched in the perpendicular attack in order to minimise the antibonding interaction between the electrons at centres 1 and 2.

This interpretation is applicable also to "intramolecular" reactions such as the [1, 2]-migration. The transition state for the concerted mechanism is described by the minimum on the η axis in Fig. 2a and can therefore be reached only if the electrons of the original bond are decoupled. Thus the activation energy is high and an elongation of the bond is necessary to stabilize the transition state. The two-step (dissociation and recombination) mechanism on the other hand is favoured because in both steps only the small barriers for the linear attack have to be overcome.

Eq. (15) and Eq. (16) are explicit expressions for the curves *a* and *b* in Fig. 2c in terms of overlap integrals only. These curves represent the characteristic features of the H_3 potential energy hypersurface which are sufficient for a discussion of all reactions of this system. Thus it is possible to estimate semiquantitatively the geometries and the relative energies of the various transition states. Such data are not available from the treatment in Ref. [3] where due to the two-electron terms no explicit expressions for geometry dependences could be obtained.

For general 3C3E systems the parameter $m_{\mu\nu}$ of Eq. (7) deals with the special properties of individual centres and Eq. (10) and Eq. (12) can be used to describe the potential energy hypersurface of the 3C3E problem in the same way as Eq. (15) and Eq. (17) were used for the H_3 system. According to Eq. (12) the curve *b* is shifted to smaller η - and ξ -values as m_{23} is larger than m_{12} and m_{13} and vice

versa. Corresponding statements are valid for Eq. (10) and Eq. (11). The results for such more general radical systems are discussed elsewhere [6].

References

1. Höweler U., Klessinger M.: *Theoret. Chim. Acta* **63**, 401 (1983)
2. For an earlier related approach cf. K. Yamaguchi and T. Fueno: *Chem. Phys. Lett.* **38**, 51 (1976)
3. Bonačić-Koutecký V., Koutecký J., Salem L.: *J. Am. Chem. Soc.* **99**, 842 (1977)
4. Wolfsberg M., Helmholtz L.: *J. Chem. Phys.* **20**, 837 (1952)
5. Huzinaga S.: *J. Chem. Phys.* **42**, 1293 (1965)
6. Höweler U., Klessinger M.: *Angew. Chem.* **96**, 962 (1984)

Received November 18, 1984/January 14, 1985